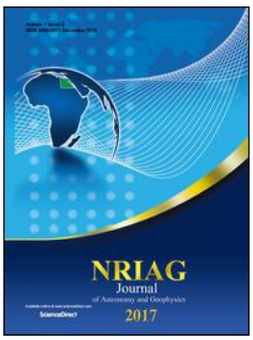

NRIAG Journal of Astronomy and Geophysics

ISSN: (Print) 2090-9977 (Online) Journal homepage: https://www.tandfonline.com/loi/tjag20

Hydrogeophysical study at an arid area: case study at Ayun Musa hot springs, Sinai, Egypt

Gad El-Qady, Safaa Shanab, Mohamed Omran, Abd-Alrahman Embaby & Hatem Aboelkhair

To cite this article: Gad El-Qady, Safaa Shanab, Mohamed Omran, Abd-Alrahman Embaby & Hatem Aboelkhair (2020) Hydrogeophysical study at an arid area: case study at Ayun Musa hot springs, Sinai, Egypt, NRIAG Journal of Astronomy and Geophysics, 9:1, 16-29, DOI: 10.1080/20909977.2019.1706834

To link to this article: https://doi.org/10.1080/20909977.2019.1706834

Published online: 08 Jan 2020.

NRIAG JOURNAL OF ASTRONOMY AND GEOPHYSICS
2020, VOL. 9, NO. 1, 16–29
https://doi.org/10.1080/20909977.2019.1706834

Hydrogeophysical study at an arid area: case study at Ayun Musa hot springs, Sinai, Egypt

Gad El-Qady[a], Safaa Shanab[b], Mohamed Omran[b], Abd-Alrahman Embaby[b] and Hatem Aboelkhair[b]

[a]National Research Institute of Astronomy and Geophysics (NRIAG), Helwan, Cairo, Egypt; [b]Geology Department, Faculty of Science, Damietta University, New Damietta, Egypt

ABSTRACT

A geoelectrical resistivity survey supported by hydrochemical analysis was managed in Ayun Musa area to detect the groundwater aquifer, differentiate the subsurface layers and estimate the groundwater quality of Ayun Musa springs. A suit of 29 vertical electrical soundings (VES) of AB/2 varying from 1 up to 1000 metres were measured in the study area to achieve the goals. Water samples were collected from ten localities in the study area. Interpretation of the VESes using 1D and 2D algorithms indicates the presence of five geoelectric units of different resistivities. The main water bearing formation related to the Lower Cretaceous represented by the fifth layer and located at depth range from 205 to 256 m below the surface. On the other hand, Interpretation of hydrochemical analysis reveals that the groundwater in Ayun Musa area is brackish in nature. The sequence of the abundance of the major ions is in the following order Na^{+}> Mg^{+2} > Ca^{+2} and Cl^{-}> SO_4^{-2}> HCO_3^{-}. This suggests active dissolution and ion exchange processes and the high chloride and sodium concentrations indicate a major influence by seawater. Generally, the groundwater samples in the study area are not suitable for domestic purposes.

ARTICLE HISTORY
Received 29 April 2019
Revised 29 November 2019
Accepted 6 December 2019

KEYWORDS
Geoelectric; 1D; 2D inversion; geochemistry; Sinai; hot springs

1. Introduction

Nowadays, establishing new urban societies and expanding the existing ones have become one of the significant priorities for the decision makers in Egypt. Together with water, energy issue is one of the most challenges faces urbanisation. The target of this strategy is essentially to reduce the dense population around the Nile valley. Ayun Musa area is subjected to many development projects, new urbanisation, oil exploration, land reclamation, and tourism. Organised planning and managing for groundwater exploration using modern techniques is carried out for suitable exploitation, protection and management of this vital resource (WWAP, 2015). Groundwater constitutes about two thirds of the freshwater resources of the world (Chapman 1996).

In this research we use the geoelectric resistivity technique among other geophysical tools as it is the most relevant exploring tool for studying and depicting the subsurface aquifer in arid areas (Asfahani 2007; Yadav and Singh 2007; Chandra et al. 2010). The geoelectrical resistivity techniques are depending on measuring the electrical resistivity of the subsurface substances, which give information about the different geological layers, structures and sometimes the conditions of the associated groundwater (Stewart 1982; Van Overmeeren 1989; Repsold 1990; El-Waheidi et al. 1992; Nowroozi et al. 1999; Meju 2005; Ibraheem et al. 2016; Othman et al. 2019, Ibraheem and El-Qady 2017).

The study area (Figure 1) is principally located in the eastern side of the Gulf of Suez, southwest Sinai between Longitudes 32° 30`and 33° 00`E and Latitudes 29° 45` and 30° 00`N.

2. Geological context

Generally, Ayun Musa area is flat, but includes a few minor topographic highs occurring at different localities in the central and eastern parts of the studied area. The stratigraphic column of this area, as inferred from some drilled wells (e.g. Ayun Musa – 2), is characterised by thick Palaeozoic rocks unconformably overlying the Pre-Cambrian basement rocks. The Mesozoic rocks (quartzite, marl, sandstone and thin limestone beds) are well represented in this area and covered by younger clay deposits of Miocene age (Said 1990; Lashin 2015).

The main surface geology is described in the geological map shown in Figure 1. The area is mostly covered by Pleistocene deposits composed of alluvium deposits and Palaeocene deposits including Esna Shale Formation, which is composed of marly shale. Different geologic units from the Lower Eocene to Upper Cretaceous cover the eastern part of the area. The Upper Cretaceous is represented by Sudr Formation, which is composed of chalk of Maastrichtian age, Duwai

CONTACT Gad El-Qady gadosan@yahoo.com; gadosan@nriag.sci.eg National Research Institute of Astronomy and Geophysics (NRIAG), Helwan, Cairo, Egypt

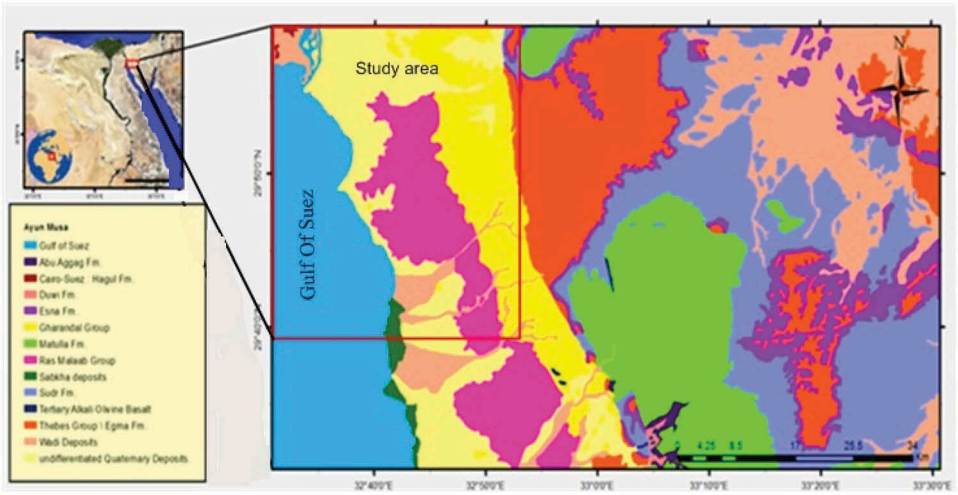

Figure 1. Geologic map of the study area (after CONCO, 1987).

Formation composed of alternated carbonate and clastic of Campanian age, Matullah Formation, which is composed of limestone of Coniacian–Santonian age (UNSECO Cairo Office, 2004).

Concerned with the geomorphologic features of the study area, several topographic highs and several wadies are existed around the study area. The high topographic features are represented by different mountains such as; Gabal Sumar, Buda and Al-Azzaz. Wadies such as Wadi Matulla, Wadi Al Jarf and Wadi Taiyba at the south of the study area, Wadi Sudr and Wadi Wardan at the west, Wadi Abu Alnatilah and Wadi Alsuhaymi at the north and Wadi Al Arish at the east of the study area (Figure 2).

3. Hydrogeological context

The study area is characterised by arid climatological conditions. It exhibits hot weather and low precipitation. Groundwater in central Sinai occurs in different water-bearing formations belonging to Quaternary, Neogene, Upper Cretaceous, and Palaeozoic. Groundwater gently flows from east to west, while depth to water gradually increases to east. The abstraction of the dug wells ranges between 25 and 70 m^3/h each; while the abstraction of the cased wells ranges between 40 and 60 m^3/h each (El-Bihery 2009).

The main sources of groundwater recharge in Ayun Musa area are direct rainfall and subsurface flow through the Miocene deposits from the east. The

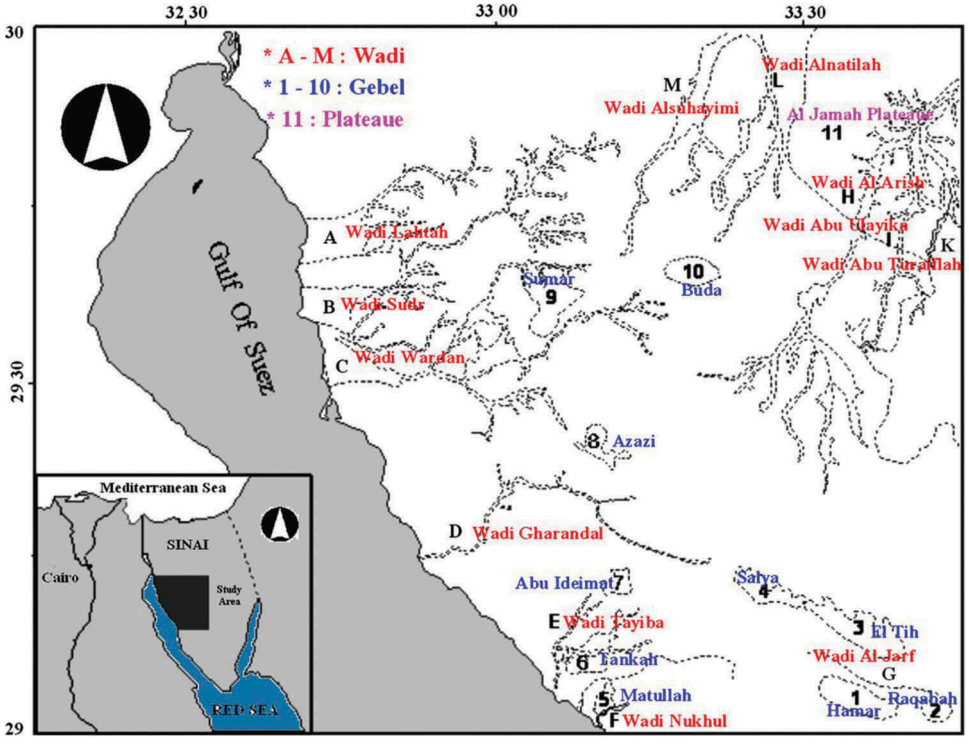

Figure 2. Geomorphologic map of the study area (after EGSMA, 1994).

amount of recharge from rainfall is about 3×10^6 m^3/year and the subsurface flow from the east accounts for 2.7×10^6 m^3/year (El-Bihery 2009). Although groundwater in most of the shallow aquifers is renewable, only 10–20% of the deep aquifers are renewable by a seeped water from the rainfall and flash floods (Elewa and Qaddah 2011).

The abstraction of groundwater is mainly due to pumping wells located in the area. The total amount of abstraction is about 6.4×10^6 m^3/year (El-Bihery 2009). The increasing groundwater abstraction from the Quaternary aquifer causes a drop in the potentiometric head as well as an increasing in the TDS in the last decade.

4. Methodology

4.1. Geoelectrical resistivity method

To fulfill the main goals of this research, a total of 29 Vertical Electric Soundings (VES) were measured in the study area (Figure 3). The field measurements were accomplished using direct current resistivity metre named McOhm manufactured by the OYO Corporation, using Schlumberger array with AB/2 ranging from 1 m to 1000 m in successive steps. At each VES station, the measured apparent resistivities are plotted versus AB/2 – spacing on bi-logarithmic paper to build the field curve for each station to have quality control on the data measurements (Figure 4).

The VES data were inverted into 1-D models using Interpex IX1D programme, which uses interpretation techniques depend on the Barnes Layer Model (Bahoi 2012) to generate resistivity and layer thickness values. The electrical resistivity contrast between lithological units enabled the delineation of geoelectric layers and identification of aquifer units. The theoretical curve that best fits the actual sounding curve specifies the thickness and resistivity of sub-surface layers beneath the respective VES station.

4.1.1. The 1D layered model

The results of 1-D inversion for the VESes were reasonable with relatively good matches between the measured and calculated curves (Figure 4). The results obtained from the one-dimensional inversion modelling of the vertical electrical sounding (VES) are used to construct the geoelectric cross sections shown in the location map (Figure 3). The geoelectric resistivity cross sections can be treated as vertical slices through the subsurface, which show the lateral and vertical subsurface resistivity distribution (Ismail 2003). These sections (Figures 5, 6) display the variations in the electrical resistivity and their corresponding

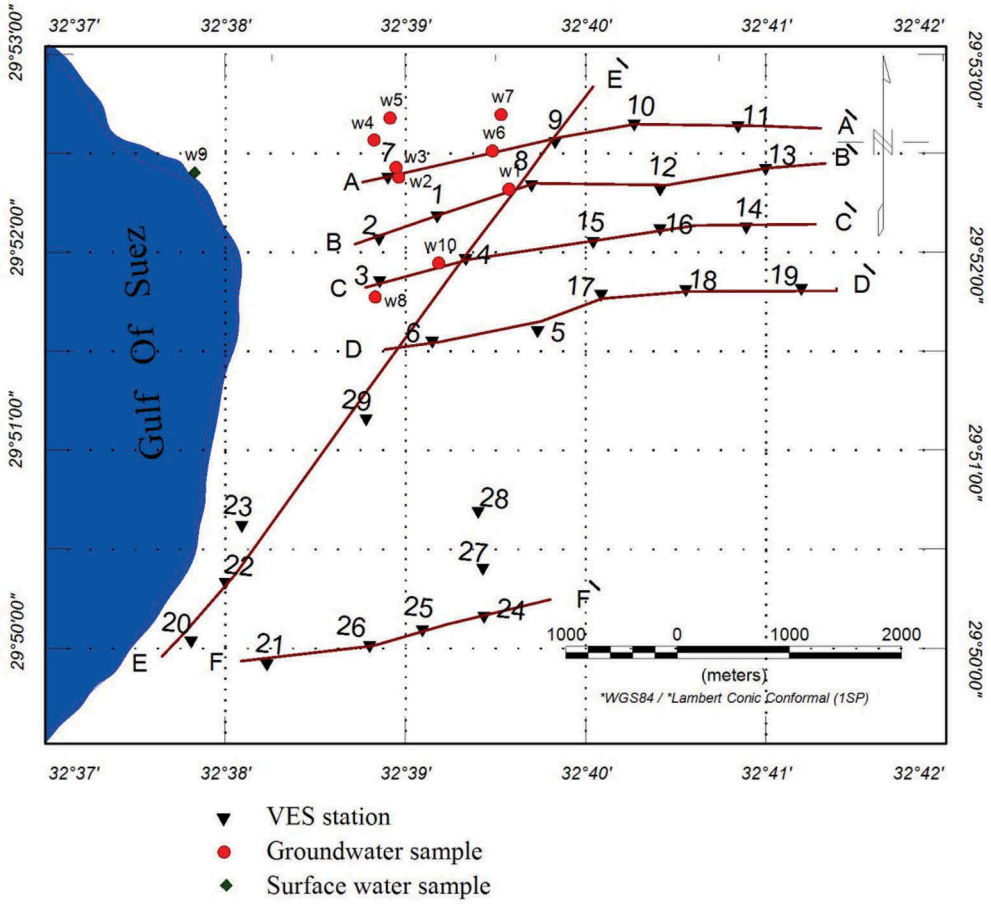

Figure 3. Location map of the VES stations and water samples.

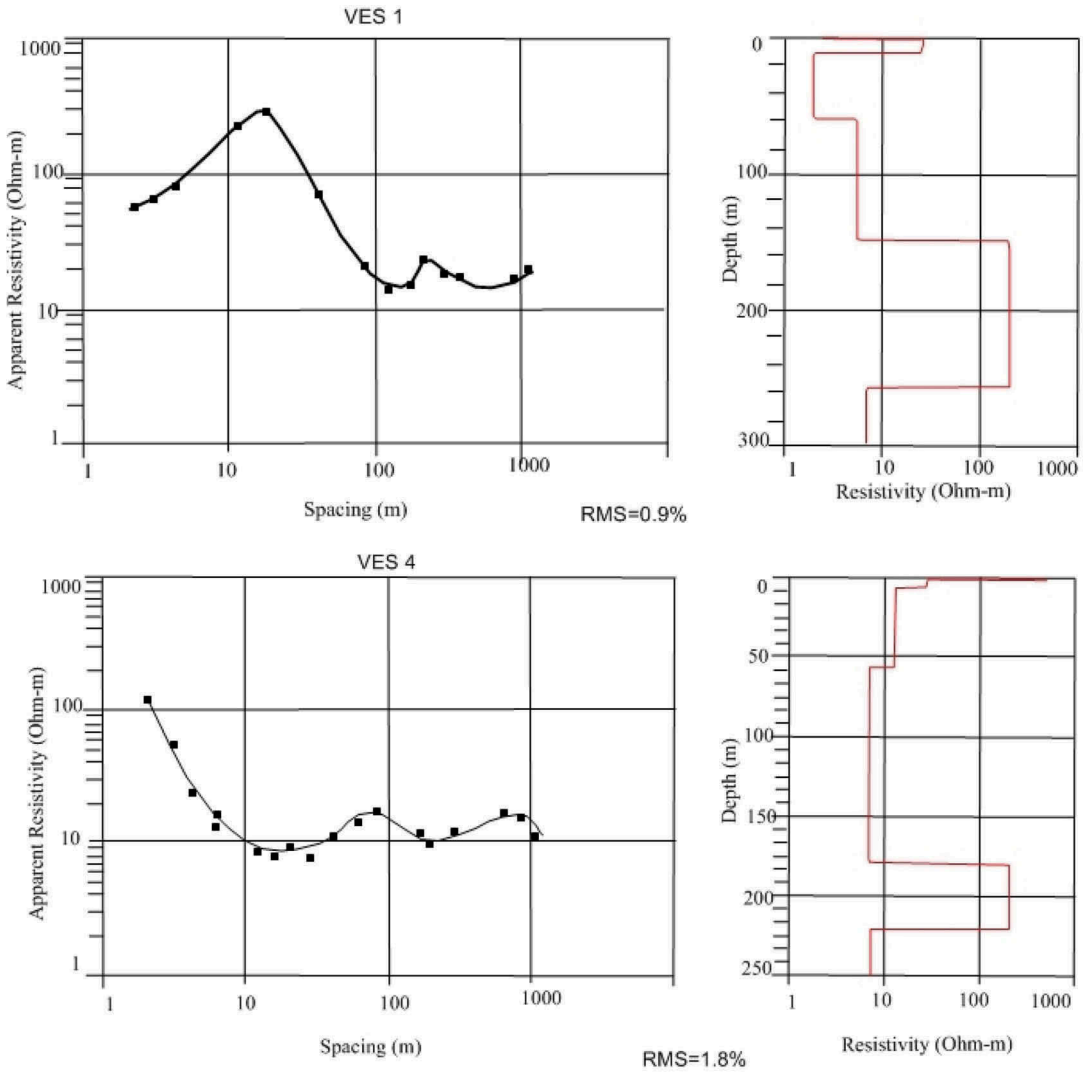

Figure 4. Examples of 1-D models of VES No. 1 and VES No. 4 using IX1D programme.

geological units and can be considered as litho resistivity stratigraphic sections (Miall 2016).

4.1.2. Two-dimensional inversion

The 2D inversion for the same data of VES stations was performed. In the 2D inversion process, the Uchida's algorithm (El-Qady et al. 1999) was used. This algorithm is based on the ABIC (Akaike Bayesian information criterion) to convert apparent resistivity values to optimum smoothness true resistivity using a finite element calculation mesh (Akaike 1980). The algorithm considers a two- dimensional earth model, where the resistivity values are varies along the X and Z, but not changed along the Y axis.

The 2D inversion of resistivity data has proven to be a vigorous tool to obtain reliable inversion results. The solution of the inverse problem must be stable to resolve complicated geological structures from the geophysical data (El-Qady and Ushijima 2001). In addition to avoid any ambiguity in 1D solution of 1D inversion of VES data we have applied the 2D inversion scheme.

Figure 7 shows the 2D cross section of the profile A-A', C- C' and E- E'. These profiles oriented E – W and NE – SW .The initial model is assumed to be a 30 ohm. m homogeneous earth, and the topography is incorporated into the modelling. The resistivities are generally low on the top layers except around VES No. 10.

It is worth to mention that the 2D inversions show high resistivity values which are not seen on the results of 1D Inversion. This indeed illustrate the capability of such inversion scheme to solve the resistivity values and depict more details in the geoelectrical structure that was not able to be inverted by 1D models.

4.2. Interpretation

The geoelectric subsurface section is discriminated into up to five geoelectrical zones of different resistivity ranges, thicknesses, depths, and hydrogeological characteristics. The examination of these geoelectric cross sections reveals the following litho-resistivity units:

The first geoelectric zone extends from the ground surface to a depth ranges from 2 to 19 m and attains a resistivity range varies from 1 to 28 ohm.m. This zone represents the superficial veneer of the aerated zone. Interpretation of this resistivity range indicates

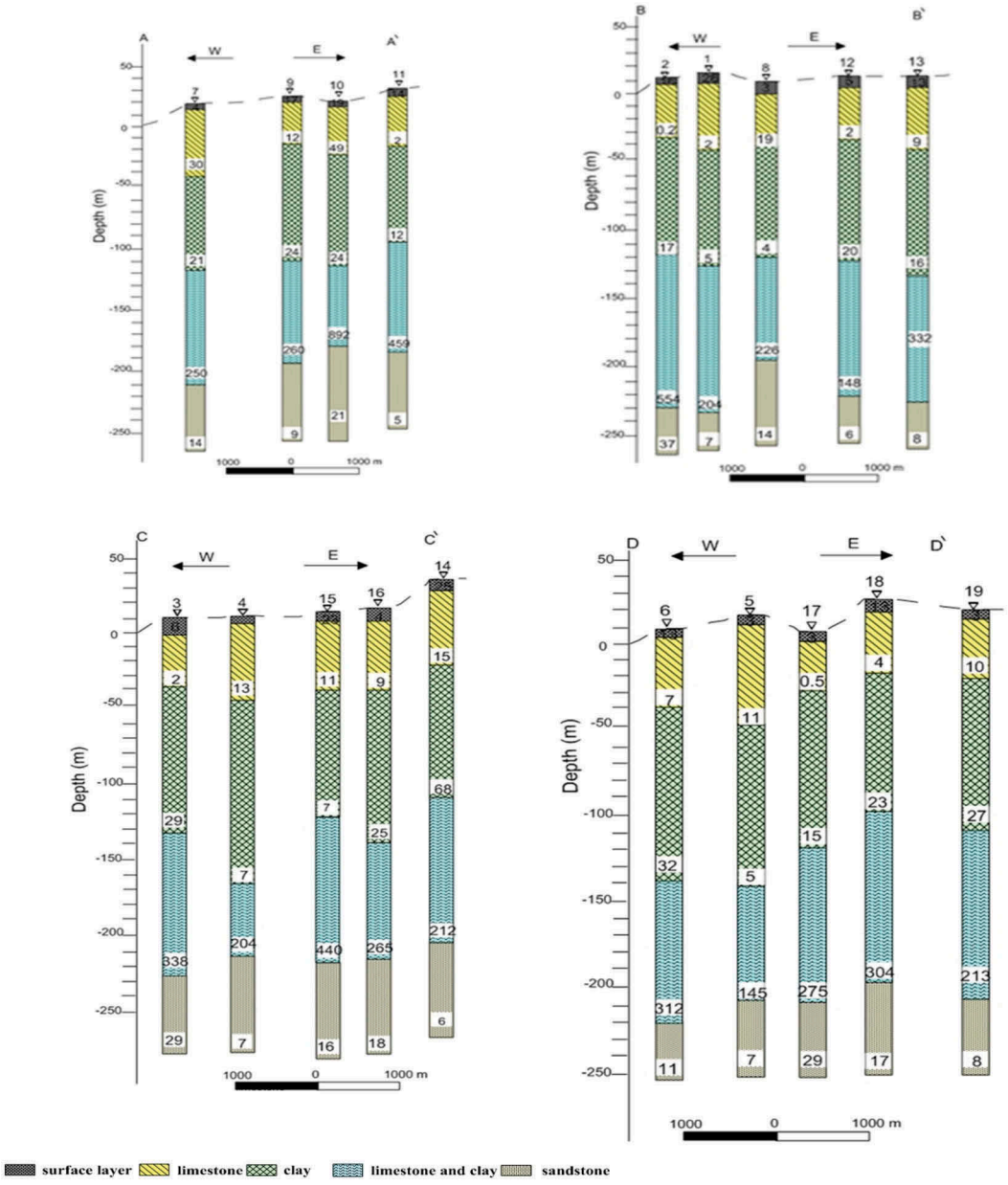

Figure 5. Geoelectric cross sections A- A′, B-B′, C- C′ and D-D′.

a heterogeneous lithology composed mainly of dry (occasionally wet) loose, friable sands of different grain sizes, mixed with shell fragments and rock debris.

The second geoelectric zone extends to a depth ranging from 39 to 70 m, with resistivity values ranging from 0.2 to 30 ohm.m. Although the resistivity values of this zone are moderate values, but according to the previous geological studies, it could be interpreted as limestone, which has thickness ranges from 20 to 63m.

The third geoelectric zone extends to depths ranging from 121 to 182 m. Its thickness ranges from 59 m to about 126 m. The resistivity of this zone ranges from 1to 68 ohm.m. Interpretation of this zone's resistivities indicates the presence of limestone and clay sediments.

The fourth geoelectric zone has a thickness ranging from 43 to 120m. This layer is characterised by high resistivities ranging from 33 to 892 ohm.m. This range of resistivities suggests hard or compact limestone and clay.

The fifth geoelectric zone is the lowermost interpreted zone, which stretches from the base of the superimpose clayey zone to the maximum depth of investigation. It has a limited range of resistivities, from 3 to 37 ohm.m. Due to the comparatively lower resistivities of this zone compared to the overlying hard limestone and clay zone (in spite of the expected relative higher salinity), it is interpreted as water saturated sandstone. This zone represents the leading aquifer in the area related to the Lower Cretaceous.

Based on the results of the geoelectric interpretation, we could construct resistivity and depth maps of the fifth geoelectric unit, which represents the water bearing layer. The true resistivity contour map of this unit (Figure 8(a)) indicates that the low resistivity values are

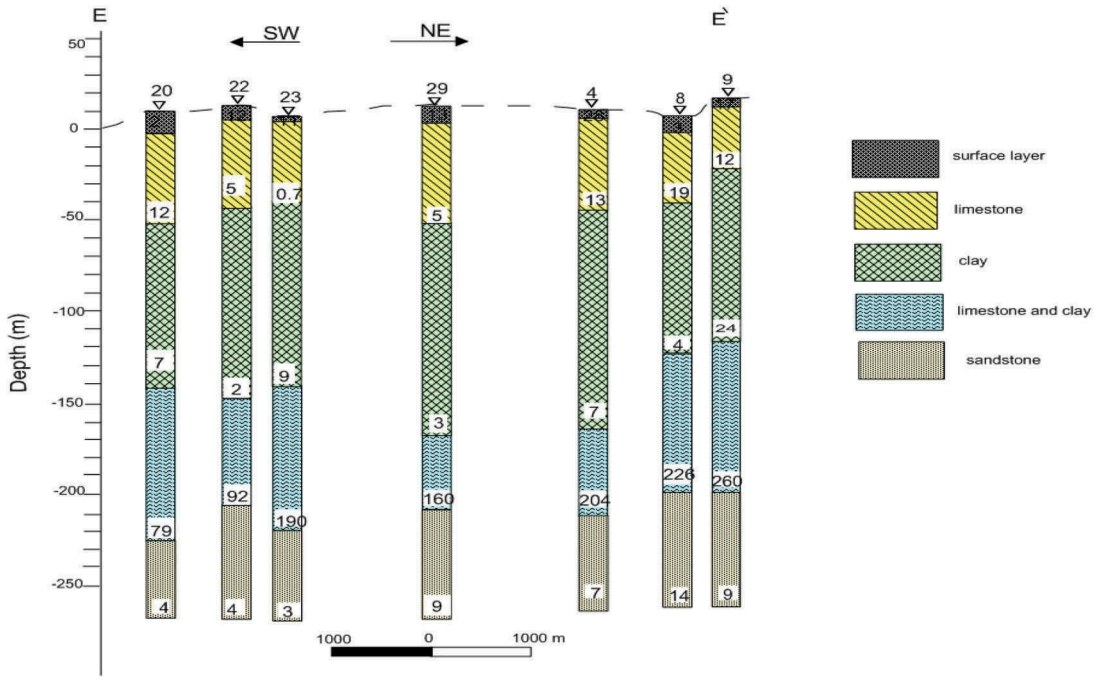

Figure 6. Geoelectric cross section E- E′.

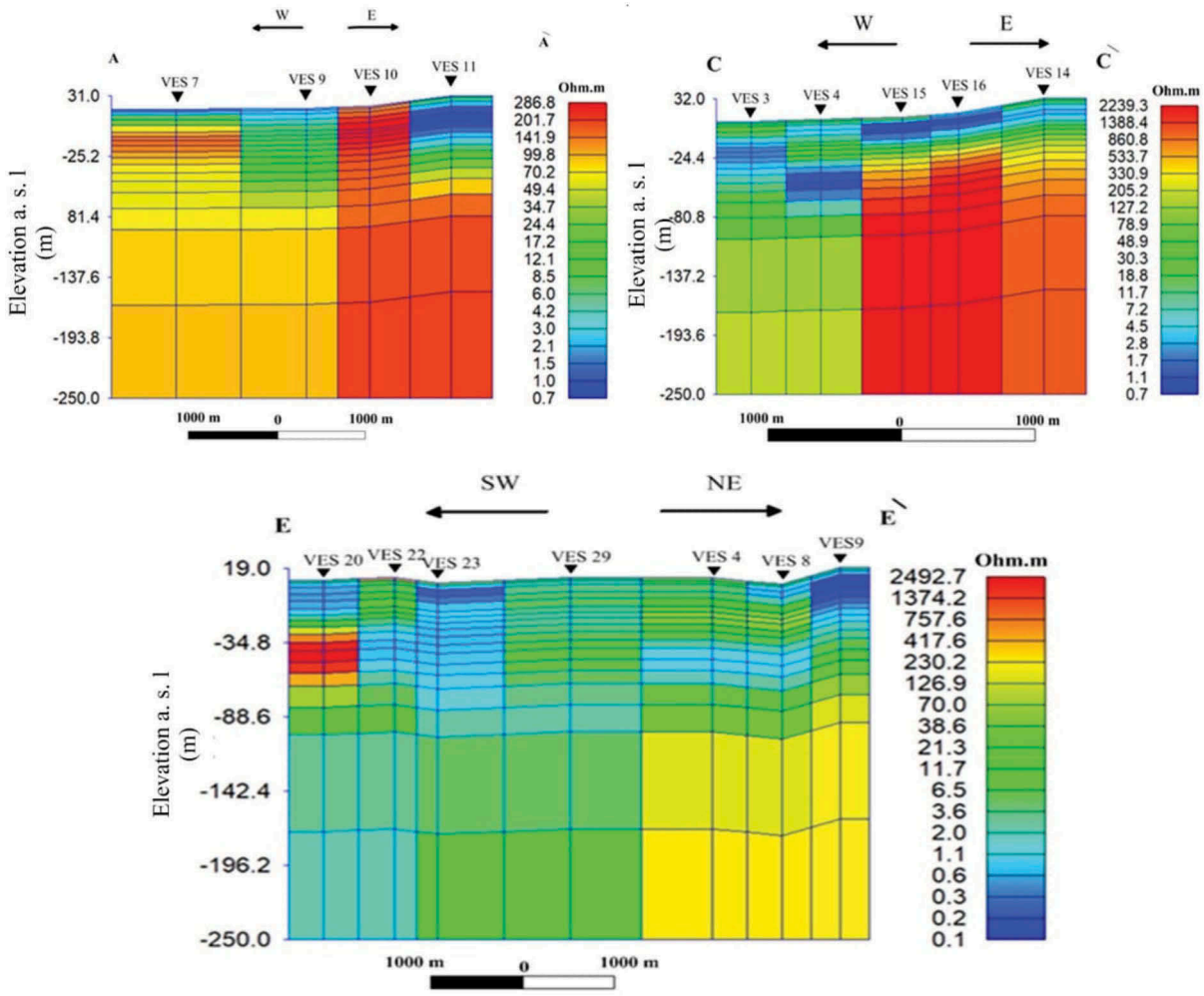

Figure 7. Two dimensional geoelectrical cross sections along profiles A- A′, C- C′ and E- E′.

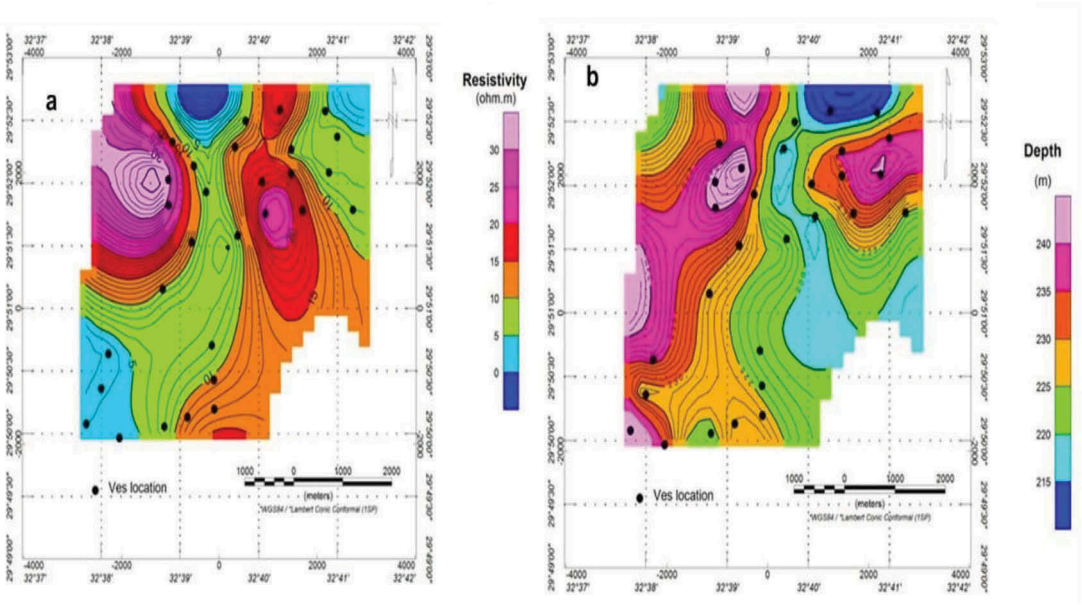

Figure 8. (a) Iso-resistivity contour map of the fifth layer, (b) Depth contour map to the fifth layer.

situated at the southwest part of the area towards the Gulf of Suez, where the high resistivity values located at the northeast. The depth to the fifth layer ranges from 205 m to 256 m. The depth contour map of this layer (Figure 8(b)) indicate that the highest value of depth is located at the east and west parts of the area, whereas the lowest value of depth is located at the north.

4.3. Geochemistrty of groundwater

Ten water samples of both surface and groundwater (Figure 3) were collected for the analyses of major cations (potassium, sodium, calcium, and magnesium) and major anions (chloride, sulphate, bicarbonate and carbonate).

Realisation the groundwater quality is important as it is the primary factor determining its suitability for drinking, domestic, agricultural and industrial purposes (Subramani et al. 2005).

The pH value of water is an indication of its quality. It is a very important factor in determining the type of water. The pH value is dependent on the carbon-dioxide-carbonate-bicarbonate equilibrium. The hydro chemical analysis of the water samples show that the pH value in the study area ranges from 7.8 to 7.9. This indicates that the groundwater of Ayun Musa area is alkaline.

Electrical conductivity (E.C.) is the ability of a substance to conduct electrical current. The ability of solution to transmit an electrical current relies on the concentration of charged ion species in the water. Thus, the measure of conductance is used to approximate the total concentration of ionic species present (Hem 1970). There is a good correlation between electric conductivity and chloride and sulphate content in a groundwater rather than (HCO_3-) concentration(Hem 1970). In the study area, the electric conductivity values range from 4.18 mmhos/cm (sample No. 7) to 15.77 mmhos/cm (sample No. 3). The total dissolved solids measurements express the concentration or the sum of all cations and anions in mg/l. TDS content of the analysed groundwater samples ranges From 2675 mg/l (sample 7) to 10093 mg/l (sample 3).

The groundwater samples were classified according to the total dissolved solids into different water classes (Table 1).

4.3.1. Distribution of major cations

The analysed groundwater samples contain potassium ranging from 52.82 mg/l (sample 8) to 256 mg/l (sample 3). Sodium represents the dominant cation in the analysed groundwater samples. It varies from 349.60 mg/l (sample 7) to 1858.40 mg/l (sample 10). The observed excess of Na^+ over K^+ is caused principally by the inflow of NaCl brines derived from seawater. Magnesium content ranges from 110.17 (sample No. 8) to 426.02 (sample No.5) mg/l. Calcium ranges from 168.40 mg/l (sample 8) 647.80 mg/l (sample 5).

4.3.2. Distribution of major anions

Chloride is one of the very important anions in most natural water (Table 2). The chloride content is important in assessing water for domestic and irrigation purpose. Chloride concentrations of the analysed

Table 1. Classification of the groundwater samples Ayun Musa area (Soni and Pujari, 2010).

Water class	TDS (mg/l)	Samples
Fresh water	0 – 1000	-
Brackish	1000 – 10,000	1, 2, 4, 5, 6, 7, 8 & 10
Saline	10,000–100,000	3

groundwater samples range from 781.00 mg/l (sample 7) to 2840.00 mg/l (sample 3). Sulphate is the second abundant anion in seawater so that it can also be used as a tracer without chemical reactions as sulphate reduction or gypsum precipitation (Richter and Kreitler 1991). Sulphate concentrations of the analysed groundwater samples range from 921 mg/l (sample 7) to 3709.44 mg/l (sample 3). The existence of bicarbonate ions in the groundwater is derived from carbon dioxide in the atmosphere, soils and by dissolution of carbonate rocks (Davis and De Weist 1966). In the study area, bicarbonate ions is in the range of about 27 mg/l.

4.3.3. Ion dominance and water types

The chemical composition of the groundwater is mainly affected by the mineralogical composition of the water bearing formation. As groundwater moves within the aquifer, dissolution increases and most of major ions normally occur (Freeze and Cherry 1979). Chloride-sodium is the main water type that represents all the collected water samples. They have solute abundances in the order Na^{+}> Mg^{+2} > Ca^{+2} and Cl^{-}> SO_4^{-2} > HCO_3^{-}.The chloride-sodium type suggests active dissolution and ion exchange processes and the high chloride and sodium concentrations indicate a major influence by seawater (Jeen et al. 2001).

4.3.4. The hypothetical salt assemblages

The combinations between major ions in the groundwater samples Ayun Musa area reveal the occurrence of the salt assemblage KCl, NaCl, $MgCl_2$, $MgSO_4$, $CaSO_4$, and $Ca(HCO_3)_2$ in samples No. 2, 4, 6 & 7. It is similar to the salt assemblage of the analysed water sample from the Gulf Of Suez (sample No. 9). According to Mowka (2009), $MgCl_2$ and $MgSO_4$ salts characterise sea water. Therefore these groundwater samples reflect a marine affinity. The rest of samples comprise the salt assemblage KCl, NaCl, Na_2SO_4, $MgSO_4$, $CaSO_4$, and Ca $(HCO_3)_2$.

4.3.5. Hydrochemical classification

The hydrochemical classification of water is a useful tool for the correlation of the various water analyses as well as development and genesis of water chemical properties. This is visually and graphically recognised in this study by the application of two main methods: Schoeller semi-logarithmic graph (1962) and Piper trilinear diagram (1944).

4.3.5.1. The semi-logarithmic graph (schoeller 1962).

The chemical analyses on this graph (Figure 9) are represented by lines, each line representing the chemical composition of a water sample. Approximated parallel lines indicate near similar compositions. This allows a visual comparison to be made between waters of different composition (Hedley 2009). The representation of the chemical composition of water samples on the semi-logarithmic graphs revealed the following (Figure 9). The majority of the collected groundwater samples falls in one main category of ionic proportion rCa+2< rMg+2< rNa+< rCl-> rSO4-2> rHCO3-. Only samples Nos. 8 and 10 have the category of ionic proportion rCa+2< rMg+2< rNa +> rCl-> rSO4-2> rHCO3-.

4.3.5.2. The trilinear diagram(piper 1944).

Piper's diagram was developed to investigate the origin of the water and the source of its dissolved salts and explain different processes affecting groundwater characters (Piper 1944). Generally, the main purpose of this diagram is to show clustering of data points to indicate samples that have similar compositions (hydrogeochemical facies). The classification of groundwater samples (Figure 10) are listed in Table 3.

5. Water quality evaluation

Water quality gives a clear picture about the usability of water for different purposes.

5.1. Evaluation of groundwater for domestic purposes

Assessment of the suitability for domestic consumption was evaluated by comparing the hydrochemical parameters of groundwater samples of Ayun Musa area with the prescribed specification adopted by ECAFE and UNESCO, (1993) (Table 4).

Water to be used for livestock and poultry, is also subjected to quality limitations of the type as those pertaining to drinking by human beings. The principle criteria for evaluating the water quality for purposes of livestock and poultry are shown in (Table 5) as determined by the National Academy of Science and the National Academy of Engineering (1972). This classification depends mainly on the total salinity value.

5.2. Evaluation of groundwater for irrigation purposes

The suitability of groundwater for irrigation is dependent on the effects of mineral constituents in the water on both the plant and the soil (Khodapanah et al. 2009). The quality standards for irrigation water are based on: 1) The total salt concentration of the water as it affects yield through osmotic effects, 2) the concentration of cations that can cause deflocculating of the clay in the soil and resulting damage to soil structure and declines in infiltration rate, and 3) the concentrations of specific ions that may be toxic to plants or that have an unfavourable effect on crop quality.

Parameters such as salinity and sodium adsorption ratio (SAR) have been used to assess the suitability of

Table 2. Hydrochemichal coefficients and hypothetical salt assemblages for the water samples in Ayun Musa area.

	Hydrochemical coefficients (ratios)				Hypothetical salt assemblages (e%)							
sample	Na^{+}/CL^{-}	Ca^{++}/Mg^{++}	SO_4–/CL^{-}	CL/HCO_3	KCl	NaCl	$MgCl_2$	Na_2SO_4	$MgSO_4$	$CaSO_4$	$Ca(HCO_3)_2$	S A R
1	0.99	0.92	0.95	157.45	6.48	44.56	0.00	5.95	22.35	20.33	0.32	12.10
2	0.74	0.92	0.91	140.00	8.95	38.59	4.70	0.00	22.56	24.83	0.37	5.52
3	0.97	0.91	0.97	200.00	8.56	42.18	0.00	7.20	22.02	19.79	0.25	13.52
4	0.81	0.92	0.90	40.67	8.30	42.01	1.61	0.00	24.22	22.59	1.28	5.78
5	0.92	0.92	0.91	397.45	7.68	44.55	0.00	3.49	23.01	21.14	0.13	12.60
6	0.80	0.89	0.93	75.43	7.50	40.97	2.96	0.00	24.25	23.64	0.68	6.18
7	0.69	0.88	0.88	36.67	9.08	36.34	7.22	0.00	21.75	24.13	1.44	4.50
8	1.18	0.93	0.94	43.33	5.44	45.45	0.00	14.88	17.74	15.32	1.17	10.42
9	0.79	0.92	0.13	495.55	6.42	70.17	11.74	0.00	0.42	11.07	0.18	52.69
10	1.05	0.99	0.97	127.33	7.26	43.34	0.00	10.96	19.25	18.79	0.40	15.11

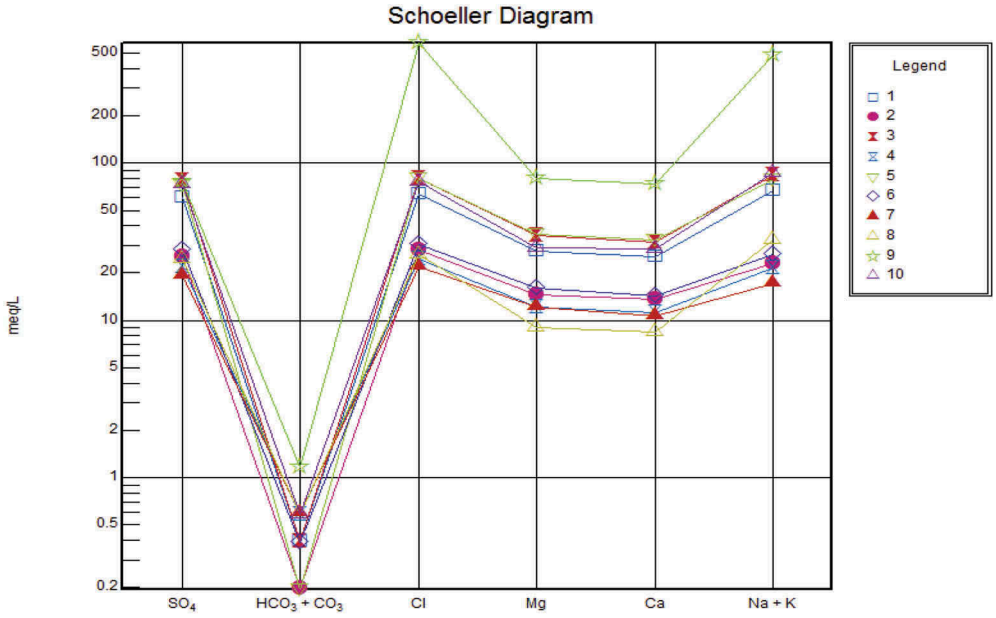

Figure 9. Semi-logarithmic representation(Schoeller 1962) of the collected water samples from Ayun Musa area, Egypt.

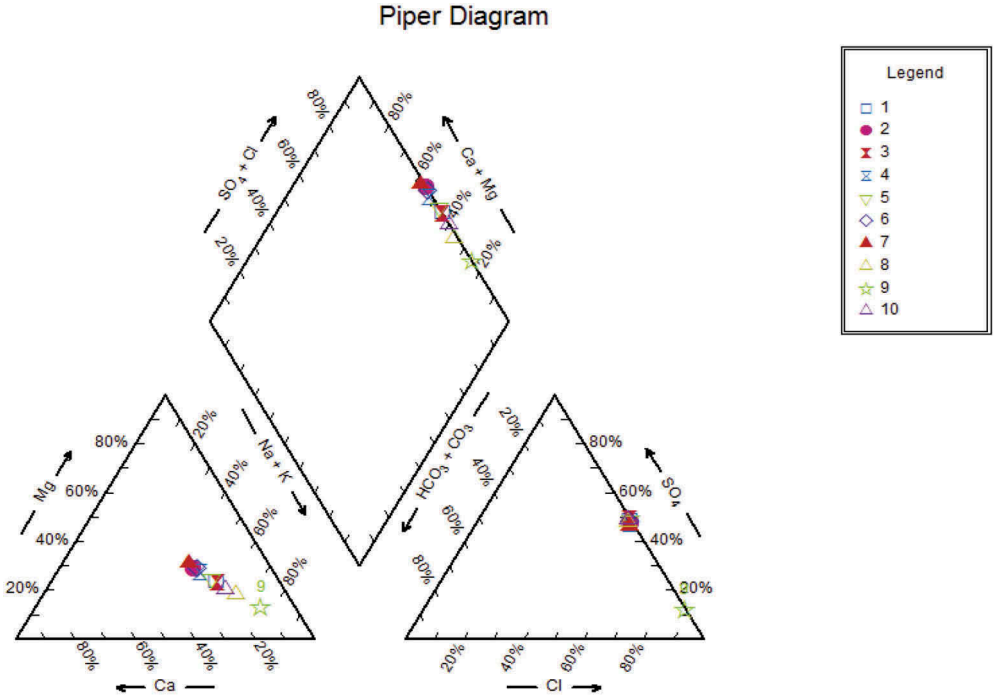

Figure 10. Plots of the analysed water samples, Ayun Musa area, Egypt, on Piper trilinear diagram.

the groundwater in Ayun Musa area for irrigation purposes (Table 2).

5.2.1. Salinity hazard

Excess salt increases the osmotic pressure of the soil solution that can result in a physiological drought condition. Even though the field appears to have plenty of moisture, the plants wilt because insufficient water is absorbed by the roots to replace that lost from transpiration (Khodapanah et al. 2009). . Salinity may reduce the yields of crops by as much as 25% without visible symptoms(Rhoades 2012). Generally, the collected groundwater samples are unsuitable for irrigation based on TDS content. Table 6 showed relative tolerance of crop plants to groundwater salinity based on EC criteria.

5.2.2. Sodium adsorption ratio (SAR)

The sodium or alkali hazard is expressed as the sodium adsorption ratio (SAR); calculated using Richards (1954) equation: $SAR = Na^{+}/[(Ca^{+2} + Mg^{+2})/2]^{1/2}$, where all ionic concentrations are expressed in

Table 3. The distribution of the analysed water samples of Ayun Musa area, on the diamond field shape of the trilinear diagram.

Area	Samples
Area (1); Alkaline earths exceed alkalis	2,4.6 & 7
Area (2); Alkalis exceed alkaline earths	1, 3, 5,8, 9&10
Area (3); Alkalinity exceeds salinity (weak acids exceed strong acids)	-
Area (4); Salinity exceeds alkalinity (strong acids exceed weak acids)	All samples
Subarea (5); Secondary alkalinity, i.e. dominance of alkaline earths over weak acids	-
Subarea (6); Secondary salinity, i.e. prevalence of strong acids over alkalis	2,4.6 & 7
Subarea (7); Primary salinity, i.e. dominance of alkalis over strong acids	1, 3, 5,8, 9&10
Subarea (8); Primary alkalinity, i.e. prevalence of weak acids over alkaline earths	-
Subarea (9); No one of the cation-anion pairs exceeds 50%	-

Table 4. The permissible limits of water used for domestic purposes (ECAFE and UNESCO, 1993).

	Permissible	Samples	Excessive	Samples	Unsuitable	Samples
pH value	7–8.5	All	8.5–9.2	-	<7 or >9.2	-
TDS	500	-	1500	-	>1500	All
Magnesium	50	-	150	4, 7 &8	>150	1, 2, 3, 5, 6 & 10
Calcium	75	-	200	8	>200	1, 2, 3, 4, 5, 6, 7& 10
Chloride	200	-	600	-	>600	All
Sulphate	200	-	400	-	>400	All

All values in mg/l except pH value.

Table 5. Guide to the use of saline waters for livestock and poultry (after National Academy of Science and the National Academy of Engineering, 1972).

TDS (mg/l)	Characters	Samples
<1000	Relatively low level of salinity. Excellent for all classes of livestock and poultry.	-
1000–2999	Very satisfactory for all classes of livestock and poultry. May cause temporary and mild diarrhoea in livestock not accustom to them or water dropping in poultry.	7
3000–4999	Satisfactory for livestock but may cause temporary diarrhoea or be refused at first by animals not accustomed to them. Poor waters poultry. Often causing water faces, increased mortality and decreased growth, especially in Turkeys.	2, 4, 6& 8
5000–6999	It can be used with reasonable safety for dairy and beef cattle, for sheep, swine and horses. Avoid the use for pregnant or lactating animals. Not acceptable for poultry.	-
7000–10,000	Unfit for poultry and probably for swine. Considerable risk in using for pregnant or lactating cows, horses or sheep, or for the young of these species. In general, use should be avoided although older ruminants, horses poultry and swine may subsist on them under certain conditions.	1, 3, 5& 10

Table 6. Relative tolerance of crop plants to groundwater salinity, Ayun Musa area, Egypt (adapted from Ayers and Westcot 1976; and (NWQMS 2000).

Classes of crops	Samples	Remarks
Class 1, Sensitive crops (EC< 0.95 mmhos/cm)	-	-
Class 2, Moderately sensitive crops (EC = 0.95–1.9 mmhos/cm)	-	-
Class 3, Moderately salt tolerant crops (EC = 1.9–4.5 mmhos/cm)	7	**Field crops**: Groundnut, rice, safflower. **Vegetables**: Beet. **Forages**: Tall fescue, barley hay, trefoil (small), harding grass. **Fruits**: Date palm.
Class 4, Salt tolerant crops (EC = 4.5–7.7 mmhos/cm)	2, 4, 6& 8	**Field crops**: Sunflower, oats, soy bean. **Vegetables**: Zucchini, broccoli. **Forages**: Bermuda grass, wheat grass. **Fruits**: Olive, peach.
Class 5, Very salt tolerant crops (EC = 7.7–12.2 mmhos/cm)	-	**Field crops**: Cotton, sugar beet, sorghum, wheat.
Class 6, Generally too saline crops (EC> 12.2 mmhos/cm)	1, 3, 5& 10	**Field crops**: Barley (grains). **Forages**: Tall wheat grass.

equivalent per million (epm). While Table 7 represents the classes of the groundwater samples in Ayun Musa area, Egypt for irrigation purposes based the value of SAR according to Fipps (1996).

The relation between SAR and salinity (Figure 11) for the analysed water samples reveals that the samples are out of range except samples No. 4&7 that located under the class C4S2 (Water of very high salinity and medium SAR). This water category is satisfactory for salt tolerant crops and soils of good permeability with special leaching.

6. Conclusions

A geophysical study comprises geoelectrical resistivity survey in terms of Vertical electrical soundings (VESs) was conducted for evaluating the subsurface setting and groundwater potentiality at Ayun Musa area. For

Table 7. The classes of the groundwater samples in Ayun Musa area, Egypt for irrigation purposes based the value of SAR according to Fipps (1996).

Classes of alkali hazard	SAR value (epm)	Remarks	Samples
Low	<10	Use on sodium sensitive crops such as avocados must be cautioned.	2, 4, 6& 7
Medium	10–18	Amendments (such as Gypsum) and leaching needed.	1, 3, 5, 8& 10
High	18–26	Generally unsuitable for continuous use.	-
Very high	>26	Generally unsuitable for use.	-

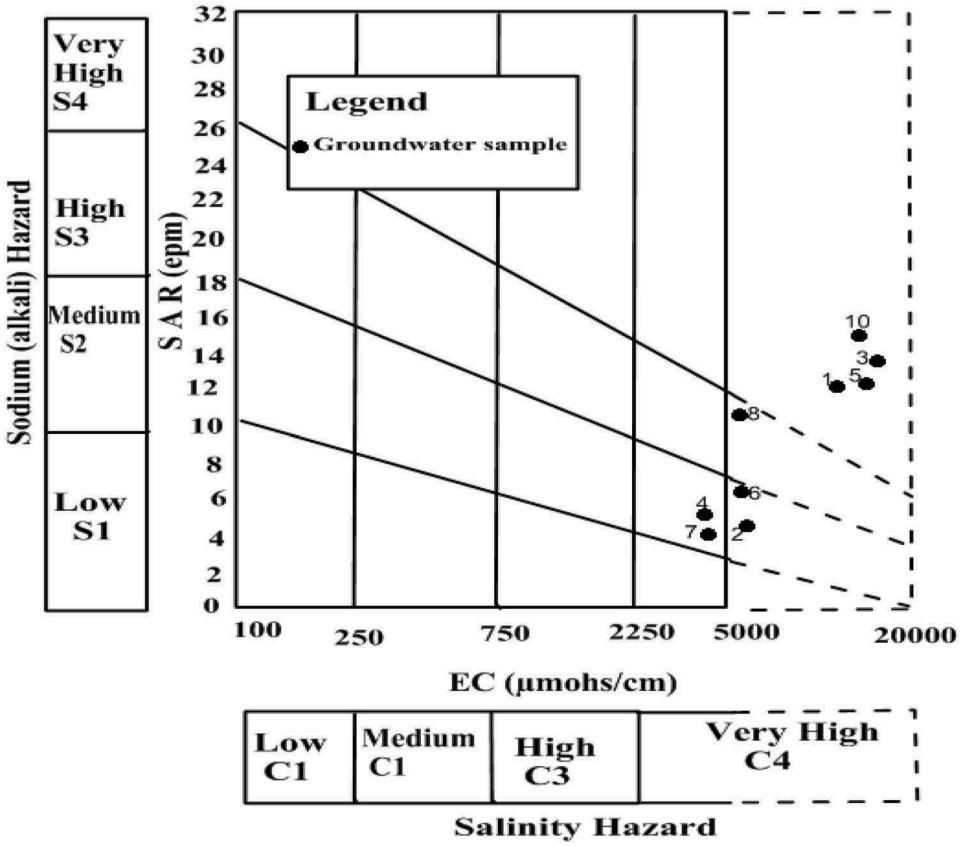

Figure 11. Classification of the examined water samples for irrigation based on USSLS (1954), Ayun Musa area, Egypt.

this target, 29 vertical electrical soundings have been conducting in the study area using Schlumberger configuration. Interpretation of the VESes indicates the presence of five geoelectric units of different resistivities. The main water bearing formation, related to the Lower Cretaceous, is represented by the fifth layer and located at depth range from 205 to 256 m below the surface. This unit has relatively low resistivity values range from 3 to 37 ohm.m. It is interpreted as water saturated sandstone.

Interpretation of hydrochemical analysis reveals that the groundwater in Ayun Musa area is brackish in nature. The sequence of the abundance of the major ions is in the following order Na+> Mg+2 > Ca+2 and Cl-> SO4-2> HCO3-. This suggests active dissolution and ion exchange processes and the high chloride and sodium concentrations indicate a major influence by seawater. Generally, the groundwater samples are not suitable for domestic purposes. Most of the samples are satisfactory for livestock but may cause temporary diarrhoea or be refused at first by animals not accustomed to them. This water needs special treatment to be used for irrigation.

Disclosure statement

No potential conflict of interest was reported by the authors.

ORCID

Gad El-Qady http://orcid.org/0000-0002-5444-1851

References

Akaike T. 1980. Likelihood and bayes procedure, bayesian statistics. Bernardo JM editor. Valencia: Valencia University Press; p. 143–166.

Asfahani J. 2007. Geoelectrical investigation for characterizing the hydrogeological conditions in semi-arid region in Khanasser valley, Syria. J A Environ. 68:31–52.

Ayers RS, Westcot DW. 1976. Water quality for agriculture. Food and Agriculture Organization (FAO), Irrigation and Drainage Paper No. 29. Rome, Italy: United Nations ; p. 97.

Bahoi A. 2012. An assessment of electrical resistivity soundings data by different interpretation techniques. International j. of biological, ecological and environmental Sci. (IJBEES), V. 1, No. 3.

Chandra S, Dewandel B, Dutta S, Ahmed S. 2010. Geophysical model of geological discontinuities in a granitic aquifer: analyzing small scale variability of electrical resistivity for groundwater occurrences, J. A Geophys. 71:137–148.

Chapman DV. 1996. Water quality assessments: A guide to use biota, sediments and water., environmental monitoring. Second ed. London UK: UNESCO, WHO, and UNEP. E & FN Spon.

CONCO/EGPC. 1987. "Geological map of Egypt", scale 1:500,000", Map sheet No. NH36NW.Klitzsch, E.;List, F. K. and poehlman, G. Editors. Berlin: Cairo (Egypt): CONCO with cooperation of the egyptian general petroleum corporation.

Davis SN, De Weist RJM. 1966. Hydrogeology. New York: Wiley; p. 463.

Economic Commission for Asia and the Far East "ECAFE" and United Nations Educational, Scientific and Cultural Organization "UNESCO". 1993. The development of groundwater resources with special reference to deltaic areas. New York: United Nations; p. 244.

Egyptian Geological Survey and Mining Authority (EGSMA). 1994. Geological and structural map of Sinai, Arab Republic of Egypt (ARE). Sheet No. 1, 3 Scale 1:250,000.

El-Bihery MA. 2008. groundwater flow modeling of quaternary aquifer Ras Sudr, Egypt. Environ Geol. 58 (2009):1095–1105.

Elewa HH, Qaddah AA. 2011. Groundwater potentiality mapping in the Sinai Peninsula, Egypt, using remote sensing and GIS-watershed-based modeling. Hydrogeol J. 19(3):613–628.

El-Qady G, Sakamoto C, Ushijima K. 1999. 2-D inversion of VES data at Saqqara archaeological area, Egypt. Earth Planets Space. 51:1091–1098.

El-Qady G, Ushijima K. 2001. Inversion of DC resistivity data using neural networks. J Geophys Prospect. 49:417–430.

El-Waheidi M, Merlanti F, Pavan M. 1992. Geoelectrical resistivity survey of the central part of Azraq basin (Jordan) for identifying saltwater/freshwater interface. J Appl Geophys. 29:125–133.

Fipps G. 1996. Irrigation water quality standards and salinity management strategies, texas agricultural extension service, Texas. College Station (Texas): A&M Univ. System; p. B–1667.

Freeze RA, Cherry JA. 1979. Groundwater. Englewood Cliffs (NJ): Prentice-Hall; p. 604.

Hedley PJ. 2009. The hydrogeochemistry of spring and Gorge waters of the Karijini National Park, Pilbara, Western Australia [MSc Thesis]. Engineering Geol., Canterbury Univ; p. 201.

Hem JD. 1970. Study and interpretation of the chemical characteristics of natural water (No. 1473). US Government Printing Office. 363p.

Ibraheem IM, El-Qady G. 2017. Hydrogeophysical investigations at El-Nubariya-Wadi El-Natrun Area, West Nile Delta, Egypt. Springer, Cham: Groundwater in the Nile Delta; p. 235–271.

Ibraheem IM, El-Qady GM, ElGalladi A. 2016. Hydrogeophysical and structural investigation using VES and TDEM: a case study at El-Nubariya - Wadi El-Natrun area, west Nile Delta, Egypt. NRIAG J Astron Geophys. 5(1):198–215.

Ismail AM. 2003. Geophysical, hydrological and archaeological invistigation in the East Bank of Luxor [Ph. D. Thesis]. Missouri-Rolla: Geol. and Geophys. Dept.; p. 211.

Jeen SW, Kim JM, Ko KS, Yum B, Chang HW. 2001. Hydrogeochemical characteristics of groundwater in a mid-western coastal aquifer system. Korea Geosci J. 5 (4):339–348.

Khodapanah L, Suliman WN, Khodapanah N. 2009. Groundwater quality assessment for different purposes in Eshtehard district, Tehran, Iran. Eur J Sci Res. 36 (4):5433–5553.

Lashin A. 2015. Geothermal resources of Egypt: country update. Proceedings World Geothermal Congress; April 19–25; Melbourne, Australia.

Meju M. 2005. Simple relative space–time scaling of electrical and electromagnetic depth sounding arrays: implications for electrical static shift removal and joint DC-TEM data inversion with the most-squares criterion. Geophys Prospect. 53:1–17.

Miall AD. 2016. Stratigraphy: a modern synthesis. Switzerland: Springer International Publishing; p. 454p.

Mowka EJ. 2009. The sea water manual: fundamentals of water chemistry for marine aquarists. Cincinnati: United Pet Group Inc.; p. 90p.

National Academy of Science and National Academy of Engineering (NAS & NAE). 1972. Water quality criteria. Rep. prepared by Committee of Water Quality Criteria at request of U.S. Environ; Washington D.C.: Protection Agency; p. 594p.

Nowroozi AA, Horrocks SB, Henderson P. 1999. Saltwater intrusion into the freshwater aquifer in the eastern shore of Virginia; a reconnaissance electrical resistivity survey. J Appl Geophys. 42:1–22.

NWQMS. 2000. Australian and New Zealand guidelines for fresh and marine water quality national health and medical research council and agriculture and resource management council of Australia and New Zealand. p. 1–2.

Othman A, Ibraheem IM, Ghazala H, Mesbah H, Dahlin T. 2019. Hydrogeophysical and hydrochemical characteristics of Pliocene groundwater aquifer at the area northwest El Sadat city, West Nile Delta, Egypt. J Afr Earth Sci. 150:1–11.

Piper AM. 1944. A graphic procedure in the geochemical interpretation of water analysis. J Am Geophys Union Trans. 25:914–923.

Repsold H. 1990. Geoelektrische Untersuchungen zur Bestimmung der Süßwasser/Salzwasser-Grenze im Gebiet zwischen Cuxhaven und Stade. Geol Jahrb. C56:3–37.

Rhoades JD. 2012. Diagnosis of salinity problems and selection of control practices: an overview. In Agricultural Salinity Assessment and Management. p. 27–55.

Richards LA. 1954. Diagnosis and improvement of saline and alkali soils. Handbook; p. 60. Washington, DC: US Department of Agriculture.

Richter BC, Kreitler CW. 1991. Identification of sources of groundwater salinization using geochemical techniques. US Environ Protection Agency document (600/2-91/064). p. 259.

Said R. 1990. The geology of Egypt. Rotterdam: A.A. Balkema.

Schoeller H. 1962. Geochemie des eaux souterraines. Rev De L'Institut Francais Du Pertole. 10:230–244.

Soni AK, Pujari PR. 2010. Groundwater Vis–vis sea water intrusion analysis for a part of limestone tract of Gujarat coast, India. J Water Resour Protect. 2:462–468.

Stewart MT. 1982. Evaluation of electromagnetic methods for rapid mapping of salt water interfaces in coastal aquifers. Ground Water. 20:538–545.

Subramani T, Elango L, Damodarasamy S. 2005. Groundwater quality and its suitability for drinking and agricultural use in Chithar River Basin, Tamil Nadu, India. Environ Geol. 47(8):1099–1110.

UNESCO Cairo Office. 2004. Geologic Map of Sinai, Egypt, Scale 1:500,000, project for the capacity building of the Egyptian Geological survey and mining authority and the national authority for remote sensing and space Sci. in cooperation with UNDP and UNESCO. Geological Survey of Egypt.

USSLS U. 1954.Diagnosis and improvement of saline and alkali soils. United States Department of Agriculture: Washington; p. 166. Agriculture Handbook No. 60.

Van Overmeeren R. 1989. Aquifer boundaries explored by geoelectrical measurements in the coastal plain of Yemen, A case of equivalence. Geophys. 54:38–48.

WWAP (United Nations World Water Assessment Programme). 2015. The united nations world water development report 2015: water for a sustainable world. Paris: UNESCO.

Yadav GS, Singh SK. 2007. Integrated resistivity surveys for delineation of fractures for ground water exploration in hard rock area. J A Geophys. 62 (3):301–312.